Precipitable water vapor characterization in the Gulf of Cadiz region (southwestern Spain) based on Sun photometer, GPS, and radiosonde data

B. Torres,[1] V. E. Cachorro,[1] C. Toledano,[1] J. P. Ortiz de Galisteo,[1,2] A. Berjón,[1] A. M. de Frutos,[1] Y. Bennouna,[1] and N. Laulainen[3]

Received 26 June 2009; revised 17 February 2010; accepted 21 April 2010; published 16 September 2010.

[1] Total precipitable water vapor (PWV) is characterized for the first time over southwestern Europe by means of ground-based measurements during the period 2001–2005. Existing data from three sites located in the Cadiz Gulf region, El Arenosillo, San Fernando, and Gibraltar, using three different techniques, Sun photometer (SP), GPS, and radiosondes, are used for the analysis. The 5 year data series gives a mean value of about 2 cm (SD = 0.7 cm) and a clear seasonal pattern. In the multiannual monthly means basis, the highest values are reached in August–September, with a mean value of 2.5–2.6 cm, whereas the lowest are obtained in January–February, with an average of 1.4–1.5 cm. The data in the three sites have been compared in order to assess regional variability. Differences could be due to real local variability but also could arise from the differences in the measurement techniques. From daily to monthly bases, water vapor behavior is similar in the three sites, with the largest differences ranging from 3% in summer to 14% in winter. Outstanding results from these analyses are the observed local minimum in July, occurring during the maximum of desert dust intrusions in the southern Iberian Peninsula, and the significant differences found between the El Arenosillo (SP) and San Fernando (GPS) measurements, related to the periodical replacement of the SP instrument at El Arenosillo. The observed differences highlight the importance of drift in each SP because of filter aging or other calibration problems. Finally, the Moderate Resolution Imaging Spectroradiometer (MODIS) near-infrared water vapor product has been compared to the data from the GPS station (San Fernando). MODIS retrieval slightly overestimates PWV in summer (5%–8%) and significantly underestimates in winter (−23%).

Citation: Torres, B., V. E. Cachorro, C. Toledano, J. P. Ortiz de Galisteo, A. Berjón, A. M. de Frutos, Y. Bennouna, and N. Laulainen (2010), Precipitable water vapor characterization in the Gulf of Cadiz region (southwestern Spain) based on Sun photometer, GPS, and radiosonde data, *J. Geophys. Res.*, *115*, D18103, doi:10.1029/2009JD012724.

1. Introduction

[2] Water vapor is one of the most important constituents of the atmosphere, playing a key role in atmospheric processes over a wide range of spatial and temporal scales, from global climatology and climate change to micrometeorology [*AGU*, 1995; *Intergovernmental Panel on Climate Change*, 2007] (available at http://www.ipcc.ch/publications_and_data/ar4/wg1/en/contents.html). The importance lies on its contribution to the global climate system as the most important greenhouse gas and on its large latent heat, which plays a fundamental role in the vertical stability of the atmosphere and in the structure and evolution of the cyclonic systems. The advection of water vapor by the general atmospheric circulation is also an essential element of the meridional energy balance. A key issue in the measurement of water vapor is its large spatial and temporal variability, which takes place on much shorter scales than other meteorological variables, such as temperature, pressure or wind speed and direction.

[3] We are interested in the monitoring and analysis of the total column water vapor content in the atmosphere defined by several parameters. One of the most common is the Integrated Water Vapor (IWV), which is the total mass of water vapor per unit area for a column of atmosphere (expressed in units of kilograms per centimeters squared). It may also be quantified as precipitable water vapor (PWV), i.e., the column thickness (in centimeters, the equivalent units to grams per centimeter squared) which the water substance would occupy if it were completely condensed and collected in a vessel of the same unit cross section at standard temperature

[1]Group of Atmospheric Optics, University of Valladolid, Valladolid, Spain.
[2]Also at Territorial Delegation of Castile and Leon, Spanish Meteorology Agency, Valladolid, Spain.
[3]Pacific Northwest National Laboratory, Richland, Washington, USA.

0148-0227/10/2009JD012724

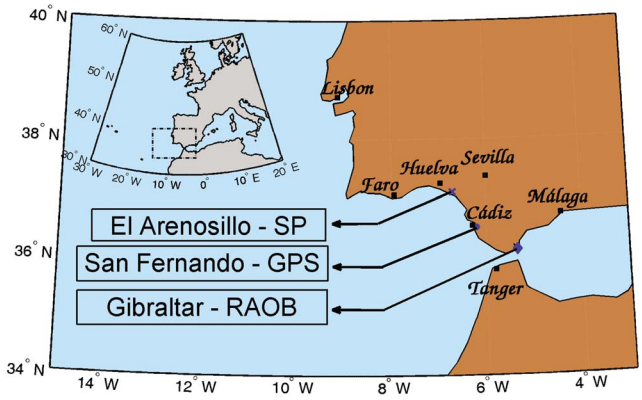

Figure 1. Map of the Gulf of Cadiz region in the southwestern part of the Iberian Peninsula showing the three stations: San Fernando (GPS), El Arenosillo (Sun photometer, SP), and Gibraltar (radiosonde observations, RAOB).

and pressure (STP). Precipitable water represents an upper limit to the total amount of precipitation that may be realizable from a given atmospheric column. PWV varies greatly both in space and time, from about 5 cm near the equator to less than 0.1 cm at the poles.

[4] A variety of instrumentation, based on different techniques and methods, has been developed in the last decades to retrieve the total vertical water vapor content in the atmosphere, from remote sensing techniques to systems that sample "in situ" air. Each technique has its advantages and drawbacks. However, an instrument which provides both good spatial and temporal resolution does not yet exist.

[5] The analysis of the PWV content is accomplished for several reasons: (1) scarce data of this quantity exist over the Iberian Peninsula, (2) an initial climatology is needed in this region, and (3) a comparison between different techniques would be useful to check or improve PWV existing data. The Atmospheric Optics Group at the University of Valladolid participates in the Aerosol Robotic Network (AERONET) since 2000. This year, a Cimel Sun photometer (SP) was installed at the El Arenosillo station, which belongs to the Instituto Nacional de Técnica Aeroespacial (Spanish Aerospace Agency), as a collaborative effort of these two institutions and the Laboratoire d' Optique Atmospherique of Lille University (France). El Arenosillo was the first AERONET [*Holben et al.*, 1998] site operating in the Iberian Peninsula, giving rise to the first routine monitoring site for atmospheric aerosols and also total precipitable water vapor from radiometric observations. Since 2006 the group is responsible for the Sun photometer calibration within the Iberian Network for Aerosol Measurements (Red Ibérica de Medida fotométrica de Aerosoles, RIMA), fully integrated in AERONET. AERONET data are generically used as ground truth for satellite remote sensing validation of water vapor [*Ferrare et al.*, 2000; *Guanter et al.*, 2008] and aerosol products [*Guanter et al.*, 2008; *Curier et al.*, 2008].

[6] The main goal of this paper is to evaluate the temporal evolution of the PWV as an initial step in establishing a climatology in the region of study. To do this we use existing data from a 5 year period, 2001–2005, obtained at three different stations in the Cádiz Gulf (southwestern Spain) with three different types of measurement systems in operation: San Fernando, equipped with a GPS receiver, El Arenosillo, with a Cimel Sun photometer (hereafter SP), and Gibraltar Airport, where radiosondes are routinely launched. We take the opportunity of the data available in these nearby sites, which are operated for a long time by different institutions, mainly military based.

[7] As a result of this analysis, we observed significant differences between El Arenosillo (SP) and San Fernando (GPS) data. The differences were related to the periodical replacement of SP instrument at El Arenosillo. Therefore we have investigated the possible drift in Sun photometer data due to filter aging or other calibration-related problems.

[8] The paper is structured as follows: Section 2 provides a short description about the characteristics of the area and the type of data obtained at each station. Section 3 deals with the methodology, where we explain the three techniques or methods used, as well as give a short review of other techniques to measure water vapor. Section 4 shows the results, including the characterization of the column water vapor in the region; the analysis of several issues of the Sun photometer data; and the colocated comparison of GPS and Moderate Resolution Imaging Spectroradiometer (MODIS) data at San Fernando. Finally in section 5 the conclusions are presented.

2. Measurement Sites and Data

[9] The study of the vertical water vapor content in the Gulf of Cádiz is carried out with the data from the GPS receiver at the station in San Fernando, the radiosonde at the Gibraltar station, and the RIMA-AERONET Cimel Sun photometer at El Arenosillo. Figure 1 shows a map of the region and the location of the three stations. The distance between stations (about 80 km between El Arenosillo and San Fernando, and 80 km between San Fernando and Gibraltar) must be taken into account in the analysis because of the spatial variability of water vapor. Since San Fernando is located in the middle and the GPS data are expected to be more reliable, the San Fernando station is taken as a reference for the analysis of regional differences among the sites. The study region has very favorable weather conditions, with an average of about 156 cloudless days and 2998 hours of sunshine per year, implying that 68% of the total time is spent in sunlight. Seventy-five percent of the days, including partly cloudy days, allow Sun photometer measurements.

[10] The GPS (Trimble 4000SSE, antenna TRM29659.00, no radome) in San Fernando, Cádiz (36.5°N, 6.2°W), belongs to Real Instituto y Observatorio de la Armada de España. It has been functioning since January 1996. This station contributes to the International GNSS Service (IGS) network, as well as to the Spanish network of the Instituto Geografico Nacional de España.

[11] The radiosondes at Gibraltar Airport (36.2°N, 5.3°W) are managed by the Meteorological Office of the United Kingdom, but data were obtained from the University of Wyoming archives (http://weather.uwyo.edu/upperair/sounding.html). It is important to note that during the study period, two different radiosonde systems were used: a Vaisala DigiCORA II (MW15) system with a sounding RS80 for the period January–May 2001; and a Vaisala DigiCORA III (MW21) with RS90 from June 2001 to December 2005. The Cimel Sun photometer at El Arenosillo (37.1°N, 6.7°W) is

Table 1. The Different Sun Photometers Installed at El Arenosillo With Their Working Periods During 2001–2005[a]

AERONET Number–Sun Photometer	Start Date	End Date
114	1 Jan 2001	30 Jul 2001
45	31 Jul 2001	27 Jan 2003
50	28 Jan 2003	12 May 2004
45b	13 May 2004	14 Dec 2005

[a]AERONET, Aerosol Robotic Network.

operated within the AERONET protocols, providing near-real-time operational products that are of publicly available at the AERONET web page. AERONET level 1.5 PWV data are used in this work.

[12] The data given from Radiosonde and GPS are limited by the specification errors given by the owner release of data to the users, but in the case of Sun photometer we are not simple users. The AERONET-RIMA network employs a rigorous and well-defined calibration and data procedure to control measurement quality. The instruments are replaced approximately every year. For this reason, there is not a fixed SP at each site, but they are rotated throughout the network. Table 1 shows the list of SPs and the dates when they were operating at El Arenosillo during the study period. Note that SP 45 completed two separate periods at this site; consequently, to avoid confusion we refer to it as SP 45b during its second term.

3. Methodology and Instrumentation

[13] Instruments based on various techniques and methods have been developed to retrieve the total vertical water vapor content in the atmosphere. Many instruments use active or passive remote sensing techniques from ground-based, satellite or aircraft platforms, while others are based on in situ methods that can be carried aloft by balloons or aircraft. Generally, ground-based remote sensing techniques provide good temporal resolution but poor spatial coverage, while the opposite is true for satellite and aircraft-based platforms. In this section we provide a description of the techniques used in this study as well as an overview of other commonly used instruments and techniques.

3.1. Radiosonde

[14] Radiosondes have been the traditional technique to measure the water vapor in the atmosphere by meteorologists at ground stations. This technique provides a vertical profile of the water vapor content. Although it has some limitations, such as the finite balloon ascent rate and maximum altitude, balloon drift during the ascent, the launch cost, etc., resulting in low spatial and time resolution, it is the oldest technique and hence has a reliable long-term data archive for most of the globe. Modern radiosondes measure relative humidity with accuracy of 3.5% [*Elliott and Gaffen*, 1991] and PWV with an accuracy of a few millimeters [*Niell et al.*, 2001]. The Vaisala radiosonde system is one of the most common systems used worldwide and the one used in our study. It is launched from Gibraltar Airport twice a day at 0000 and 1200 UTC, that also correspond with site local standard time. There are several known limitations of the Vaisala RS80 and RS90 sensors, like deviation from factory calibration and sensor time lag, especially where steep humidity gradients occur at low temperatures. For further information about the radiosonde performance under different conditions, see *Miloshevich et al.* [2006], and references therein.

3.2. GPS Systems

[15] The GPS method is based on the time delay of electromagnetic waves transmitted from a constellation of GPS satellites caused by the slowing of the propagation speed of the waves as they pass through the troposphere. The delay in signal arrival time can be expressed as an equivalent increase in travel path length (in centimeters), the zenith total delay (ZTD). ZTD consists of two parts, ZTD = ZHD + ZWD, where the zenith hydrostatic delay (ZHD) is produced by the total air mass and the zenith wet delay (ZWD) arises from water vapor [*Bevis et al.*, 1992; see *Wang et al.*, 2007], and references therein. The ZHD is calculated from the atmospheric pressure at the GPS antenna height corrected by gravity.

[16] The integrated water vapor (IWV) is calculated by multiplying the ZWD by a conversion factor $f(T_m)$, IWV = $f(T_m)$ZWD, which is a function of the mean atmospheric temperature, T_m, as estimated by the surface temperature. The proliferation of GPS receivers offers the possibility of a high spatial and temporal resolution network for measuring water vapor columnar content. Total precipitable water vapor (PWV) or integrated column water vapor (IWV) can be estimated by the GPS network data with a temporal resolution of minutes and with an accuracy better than 0.15 cm [*Duan et al.*, 1996; *Wang et al.*, 2007]. GPS receivers collect data every second and different institutions provide tropospheric delay legacy product ZTD integrated over various time ranges [*Byun et al.*, 2005]. For this study it has been used the tropospheric delay legacy product ZTD of IGS calculated every 2 hours [*Gendt*, 1998]. The quality of the PWV data produced by GPS techniques has been proved by a number of intercomparison studies [*Revercomb et al.*, 2003; *Van Baelen et al.*, 2005; *Sapucci et al.*, 2007; *Bokoye et al.*, 2007].

3.3. Sun Photometer

[17] Various radiometric instruments are used to determine PWV, i.e., based on the measurement of electromagnetic radiation over a broad spectrum from the visible, through the infrared and into the microwave regions. Microwave radiometers [*Westwater et al.*, 2006; *Liljegren et al.*, 1999] (available at http://www.arm.gov/publications/proceedings/conf09/extended_ abs/liljegren3_jc.pdf) use the interaction of an emitted microwave signal with the atmosphere to retrieve the water vapor, while infrared radiometers rely on measuring the thermal longwave radiation emitted by the atmosphere.

[18] Traditional radiometers [*Michalsky et al.*, 1995], and spectroradiometers [*Cachorro et al.*, 1987, 1998] are based on solar radiation measurements. In particular, Sun photometer technique is based on the measurement of solar spectral transmittance through the atmosphere in a strong water vapor absorption band [*Thome et al.*, 1992; *Bruegge et al.*, 1992; *Schmid et al.*, 1996; *Smirnov et al.*, 2000; *Bokoye et al.*, 2007], and references therein. In the case of the Cimel CE 318, the data are obtained from the modeling of the water vapor transmittance T_w in the 940 nm channel, after correcting for Rayleigh scattering and aerosol optical depth

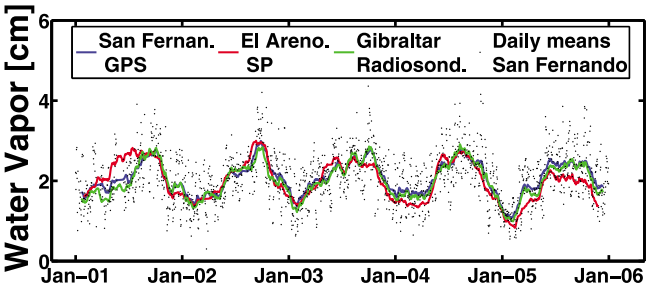

Figure 2. Time series of mean daily water vapor values given by San Fernando station data from January 2001 to December 2005. Solid lines represent a 35 point smoothed moving median from the three station data: San Fernando (blue line), El Arenosillo (red line), and Gibraltar (green line).

transmittances, T_R and T_a (see more details in the work of *Cachorro et al.* [1998] and *Bokoye et al.* [2007]):

$$T_W = VR^2 / V_0 T_a T_R,$$

where V_0 is the extraterrestrial solar irradiance (or signal) which is also the calibration constant of the Cimel photometer. V is the irradiance (or signal) measured by the SP at 940 nm. R is the Earth-Sun distance in astronomical units. T_w is modeled in the AERONET algorithm by two parameters, a and b, that depend on the filter spectral response:

$$T_W = \exp\left[-a(m \cdot IWV)^b\right],$$

where m is the water vapor air mass factor. The algorithm and methods are based on the work of *Bruegge et al.* [1992]. Additional details may be found in the work of *Holben et al.* [1998, 2001] and *Smirnov et al.* [2004].

[19] The Cimel SP obtains data about every 15 min during daytime if the solar path is free of clouds. The error associated to this technique depends on the error of the calibration constant Vo and on the modeling of the water vapor transmittance (the contribution of Rayleigh scattering and aerosols is generally much lower). According to AERONET [*Holben et al.*, 1998; *Smirnov et al.*, 2004; *Bokoye et al.*, 2007] the PWV retrieved for this technique is accurate to about 10%. However, the modeling of the 940 nm water vapor band is not straightforward because of the contribution of continuum water vapor absorption [*Cachorro et al.*, 1998; *Ingold et al.*, 2000].

[20] Note that the sampling frequencies of the three methods are different. This fact must also be taken into account in the statistics of the regional analysis. The diurnal variability of the water vapor, analyzed in section 4.3, clearly highlights this issue.

3.4. Satellite and Other Techniques

[21] A number of satellite sensors based on passive or active radiometric instruments is applied to retrieve PWV. These techniques provide good spatial but poor temporal resolution, typically with one or two overpasses per day. Many comparisons of data collected from these systems have been made, i.e., MODIS/Aqua-Terra [*Gao and Kaufman*, 2003], SCIAMACHY [*Noël et al.*, 2005] and MERIS [*Li et al.*, 2003; *Lindenbergh et al.*, 2008; *Guanter et al.*, 2008], ENVISAT, GOME/ERS-2 [*Burrows et al.*, 1999; *Lang et al.*, 2007], and recently GOME-2/Mettop [*Noël et al.*, 2008]. There are also radiometer systems retrieving the water vapor profiles using longwave infrared or microwave spectral ranges, such as the old TIROS Operational Vertical Sounder (TOVS; http://wdc.dlr.de/sensors/tovs/) [*Arbelo et al.*, 1995] and the more recent ATOVS system (http://wdc.dlr.de/sensors/tovs/), composed of various sensors, including the next-generation High Resolution Infrared Radiation Sounder, the Advanced Microwave Sounding Unit on board NOAA series satellites, and Aqua (http://aqua.nasa.gov/about/instrument_amsu.php) [*Buehler et al.*, 2008]. Other new-generation sensors, such as the Atmospheric Infrared Sounder (http://aqua.nasa.gov/about/instrument_airs.php; http://www-airs.jpl.nasa.gov/) [*Gettelman et al.*, 2006] on Aqua, use both visible and infrared bands for PWV retrieval. The Infrared Atmospheric Sounder Interferometer on Mettop is based on a different measurement principle: Michelson interferometry [*Liu et al.*, 2008]. Besides its large spatial coverage with more or less efficacy over ocean or land, it provides the water vapor profile and the total content as the integration of atmospheric profile (like radiosondes) though with low temporal resolution.

[22] Finally, we also mention active systems, such as lidar [*De Tomasi and Perrone*, 2003; *Machol et al.*, 2004; *Whiteman et al.*, 2006; *Flamant et al.*, 2003], which provides water vapor profiles with different vertical and spatial resolutions and horizontal coverage, depending on internal characteristics of the system and if they are installed in a given station or onboard a satellite platform. These systems are more useful for detailed studies about the vertical structure of water vapor in the atmosphere with the advantage of a higher temporal resolution than radiosondes or satellites radiometric sensors.

4. Results and Discussion

[23] The first part of this section deals with a general analysis of the temporal evolution and seasonal behavior of PWV for the three locations during the study period. In spite of the different measurement time scales for each technique, the results show that we can derive representative features of the area. The second part gives a general analysis about the agreement between these three techniques and the last parts reports on a more detailed comparison with more restricted data sets, but with a higher temporal resolution. Individual GPS measurements were compared with concurrent SP observations (obtained with the several different Cimel SPs installed at the El Arenosillo station) to obtain an estimate of SP stability. In addition, the two daily measurements obtained from the Radiosonde (at 0000 UTC and 1200 UTC) are compared with the GPS data (at 2300 UTC and 0100 UTC or 1100 UTC and 1300 UTC, respectively) to compare any different behavior for day or night observations. To finish the result section, a comparison between the GPS and the MODIS precipitable water vapor is carried out for the 5 year data set.

4.1 Temporal Evolution and Seasonal Behavior of PWV

[24] Figure 2 shows the PWV time series of San Fernando (GPS data) over the period 2001–2005, along with a 35 day

Table 2. Water Vapor Statistics for El Arenosillo (SP), San Fernando (GPS), and Gibraltar (RAOB) Stations in the Gulf of Cadiz Area in the Period 2001–2005[a]

	Data	Days	Mean	SD	Median	Max	Min	Percentile 10	Percentile 90
El Areno (SP)	40470	1501	1.93	0.72	1.88	5.11	0.21	1.02	2.87
San Fernan. (GPS)	20315	1701	2.07	0.64	2.06	4.36	0.30	1.23	2.88
Gibraltar	3569	1809	2.01	0.69	1.95	4.27	0.36	1.14	2.95

[a]Abbreviations are as follows: RAOB, radiosonde observations; SP, Sun photometer.

smoothing curve of the three measurement sites. The scatter of data is ranging from about 0.5 cm in winter to about 4 cm in summer, and there are significant year-to-year differences. All three sites show a generally similar behavior, with remarkable disagreements in some periods that will be analyzed later.

[25] Table 2 gives the statistics for the three data sets based on daily averaged data. The mean value is about 2.0 cm, ranging from 0.21 to 5.1 cm. El Arenosillo (SP) has the highest standard deviation. Note that the second column reports the total number of measurements of each data set and the third column gives the number of days used for the statistics. In general, San Fernando (GPS data) shows the highest values, followed by Gibraltar (radiosonde) and El Arenosillo (SP). This is not always true on a monthly basis, as can be seen in Table 3 and Figures 3 and 4. This is discussed in more detail below. All figures show a clear seasonal behavior for the three sites, with a maximum in summer and a minimum in winter.

[26] Figure 3 gives the time series of monthly mean values at the three locations, GPS, SP and Radiosonde, with similar standard deviations (bars not shown) varying about 0.2–0.7. The changes of SP instruments at El Arenosillo are highlighted by vertical dotted lines. See the low values in 2005 in comparison to the other years and the large deviation of SP values. Figure 4 shows the multiannual monthly mean, with standard deviations of about 0.4–0.7 (see Table 3).

[27] From Table 3, the annual cycle has a peak of about 2.5–2.6 cm in August at El Arenosillo and Gibraltar, and in September at San Fernando. The winter minimum is about 1.3–1.5 cm and occurs in January–February, depending on the site. The seasonal behavior was already observed in other studies over the Iberian Peninsula, such as in north central Spain (continental climate) [*Cachorro et al.*, 1998] using spectroradiometer data, or at the Mediterranean coast [*Estellés et al.*, 2007] using Cimel SP data. This is consistent with the general behavior for continental and maritime midlatitudes [*Wang et al.*, 2007; *Lang et al.*, 2007].

[28] We note that two anomalies in the seasonal cycle are shown in the data from all stations, namely, relative local minima in April and July. A more detailed analysis using only San Fernando–GPS data over a longer time period (1996–2005) for the interannual average shows that the observed April minimum disappears, whereas the July one does not. The former is, thus, an effect of the time limited database.

[29] It was shown recently that July has a maximum number of Saharan dust events [*Toledano et al.*, 2007b, esp. Figures 3, 5, and 10] in this region, with occurrence up to 33% of days. Furthermore, the type of Saharan dust events in summer is different from the rest of the year. The desert intrusions reach the Iberian Peninsula under four different weather situations (for details, see *Rodríguez et al.* [2001] and *Toledano et al.* [2007b]). The most common in summer is named North African High at high Altitude (NAH-A) and is the driest type, because the air mass reaches the Iberian Peninsula directly from Africa. The other meteorological situations imply longer trajectories and overpass the Mediterranean or Atlantic areas. We suggest that the direct trajectory at altitudes between 1000 and 3000 m could explain this unusual minimum. Studies from stations in the Iberian Peninsula confirm this behavior [*Ortiz de Galisteo et al.*, 2008], with a decreasing gradient from south to north corresponding to a decrease of the frequency of desert dust intrusions.

[30] The PWV annual means remained relatively constant and the differences between San Fernando and Gibraltar were within 5% over the 5 year period. The El Arenosillo values show larger variations (about 25%). This suggests analyzing

Table 3. Multiannual Monthly Precipitable Water Vapor Values for the Different Techniques in the Gulf of Cadiz Area in the Period 2001–2005 and Monthly Differences Taking San Fernando (GPS) as a Reference[a]

	Mean (SD)			Difference	
	El Areno (SP)	San Fernan. (GPS)	Gibraltar (RAOB)	El Areno–San Fernan. (%)	Gibraltar–San Fernan. (%)
Jan	1.35 (0.52)	1.54 (0.55)	1.42 (0.52)	−0.19 (−12.36)	−0.12 (−7.88)
Feb	1.39 (0.49)	1.53 (0.46)	1.44 (0.48)	−0.14 (−9.20)	−0.09 (−6.07)
Mar	1.70 (0.55)	1.84 (0.53)	1.74 (0.49)	−0.15 (−7.96)	−0.10 (−5.34)
Apr	1.68 (0.53)	1.74 (0.43)	1.62 (0.42)	−0.07 (−3.80)	−0.12 (−6.84)
May	2.10 (0.62)	2.01 (0.51)	1.90 (0.49)	+0.09 (4.51)	−0.12 (−5.73)
Jun	2.45 (0.56)	2.38 (0.45)	2.25 (0.52)	+0.07 (3.13)	−0.13 (−5.45)
Jul	2.37 (0.69)	2.26 (0.51)	2.26 (0.61)	+0.11 (5.06)	−0.00 (−0.19)
Aug	2.53 (0.55)	2.55 (0.47)	2.60 (0.62)	−0.02 (−0.71)	0.05 (2.11)
Sep	2.50 (0.68)	2.59 (0.56)	2.58 (0.59)	−0.09 (−3.47)	−0.02 (−0.59)
Oct	2.35 (0.66)	2.57 (0.65)	2.53 (0.68)	−0.22 (−8.42)	−0.04 (−1.47)
Nov	1.74 (0.65)	1.96 (0.57)	1.90 (0.64)	−0.22 (−11.37)	−0.06 (−3.19)
Dec	1.59 (0.53)	1.84 (0.53)	1.77 (0.54)	−0.25 (−13.74)	−0.07 (−3.98)

[a]The multiannual monthly mean is computed from daily average values (not over a monthly mean). The last two columns are the simple difference of the values of the first columns. Monthly differences are in centimeters. Percentages are given in parentheses.

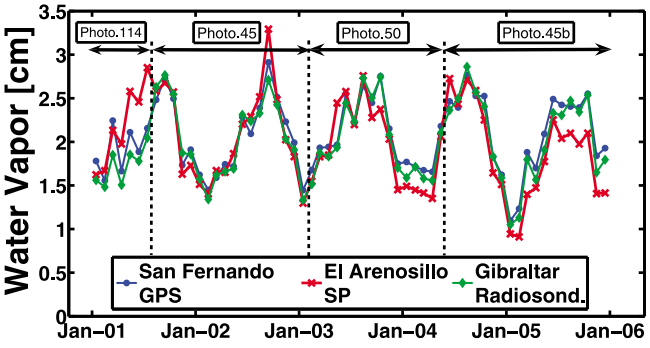

Figure 3. The time series of monthly means of water vapor during the period 2001–2005 for data collected at the three stations. Dotted lines indicate a change of SP.

in detail the PWV derived with SP at El Arenosillo and that obtained with GPS in San Fernando (see section 4.3).

[31] Finally the diurnal variation of the PWV for each site has been analyzed. For this purpose, water vapor anomaly has been calculated for each measurement by subtracting the corresponding daily mean. These anomalies have been averaged for each hour interval and the results are shown in Figure 5a. The GPS at San Fernando provides 24 hour monitoring, whereas at El Arenosillo there is only information during daylight hours. At Gibraltar only the two single radiosondes at 0000 UTC and 1200 UTC are available, therefore no information could be inferred from the radiosonde diurnal anomalies. However, it should be noted that radiosonde mean values are similar to those at San Fernando at 0000 UTC and significantly lower at 1200 UTC, as will be discussed in the next section.

[32] The GPS data at San Fernando indicate a slight increase during the morning until 1100 LT and decrease in the afternoon. The amplitude of this diurnal cycle is in average about 0.12 cm. The night minimum and morning increase of PWV follows the temperature pattern, but the quick decrease in the afternoon does not. The diurnal cycle at El Arenosillo has smaller amplitude (0.08 cm) and different pattern, showing an increase during the daylight hours that follows the temperature cycle. Furthermore, the diurnal cycle at El Arenosillo is very similar to the average over the Spanish

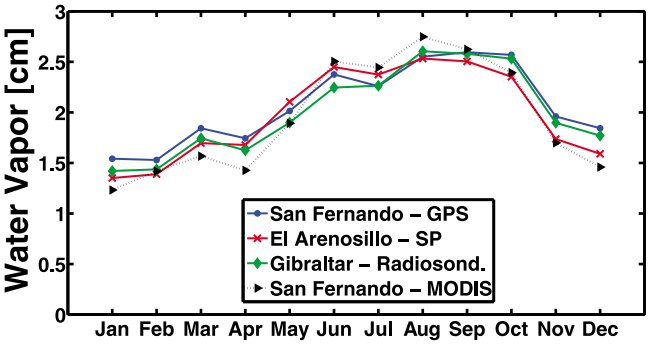

Figure 4. Interannual mean of water vapor during the period 2001–2005 for the three stations: San Fernando, El Arenosillo, and Gibraltar. The dotted line presents the interannual mean of water vapor obtained from Moderate Resolution Imaging Spectroradiometer near-infrared data.

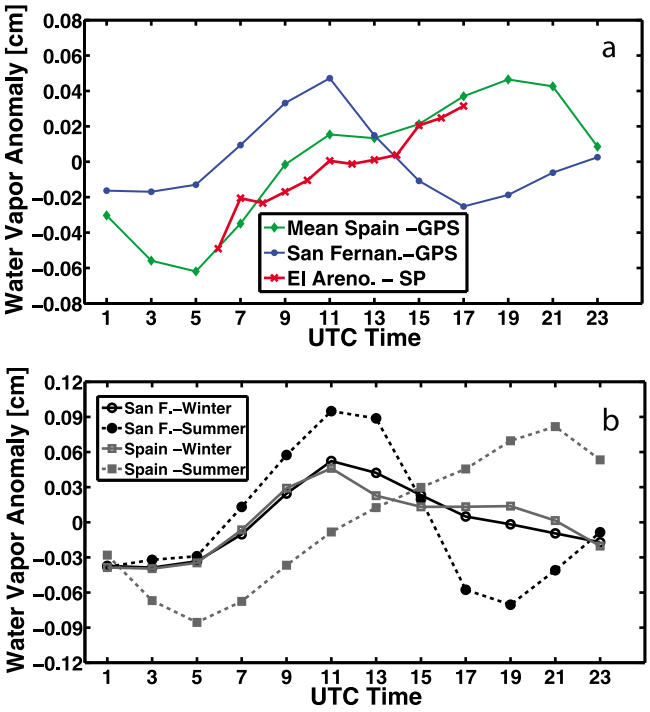

Figure 5. (a) Diurnal water vapor anomaly at San Fernando, El Arenosillo, and mean anomaly of 11 Spanish GPS sites. (b) Diurnal water vapor anomaly in winter and summer at San Fernando and the mean over Spain.

territory, calculated as the mean of 11 GPS sites in Spain [*Ortiz de Galisteo et al.*, 2010], whereas San Fernando data show a different feature.

[33] A more detailed analysis has been accomplished with the GPS data, extracting separately the diurnal cycle in the winter and summer seasons (Figure 5b). The amplitude of the diurnal cycle is doubled in summer (0.17 cm) as compared to winter (0.09 cm). The patterns are also different. Intermediate values are found in spring and fall (not shown). As can be seen, the diurnal cycle in winter in San Fernando is very similar to the average over the Spanish territory, but this similarity is not observed in summer, when the cycle at San Fernando is clearly different than the mean over Spain [*Ortiz de Galisteo et al.*, 2010]. In summer the breeze regime is stronger, as well as the solar insolation, the evaporation, and the convection. These factors, strongly conditioned by the location near Gibraltar strait, dominate the diurnal pattern in summer, whereas in winter the temperature diurnal cycle seems to be the predominant factor. Other factors, like changes in air mass, are not significant in the long term for the diurnal anomaly, since the arrival of fronts, etc. can occur at any time in the day.

4.2. Analysis of Regional Variability

[34] It is necessary to check whether the three locations are part of the same water vapor regime or not. Figure 6 shows the correlation between El Arenosillo and San Fernando (top) and Gibraltar and San Fernando (bottom) for concurrent, daily averaged measurements during the day. Note that SP observations are only available during daytime. The El Arenosillo–San Fernando comparison gives a slope of 1.002, with an intercept of −0.04 cm, a correlation coefficient

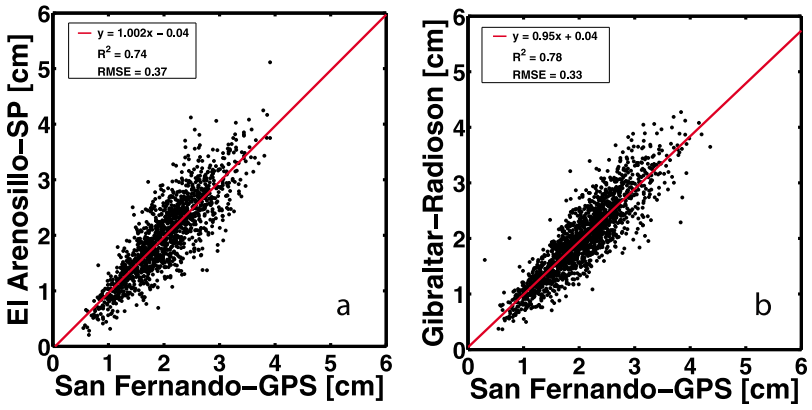

Figure 6. Regression lines and associated parameters of the comparison between (a) the data obtained in San Fernando and El Arenosillo and (b) the data from San Fernando and Gibraltar. The points are daily averaged values based on concurrent measurement times during the day for each station.

R^2 = 0.74 and a RMSE = 0.37. These values demonstrate good agreement between both stations from a climatological point of view. However, on a daily basis, differences can be larger than 50%. The comparison between Gibraltar and San Fernando is similar to the first one, with no substantial differences. These values are in agreement with other comparisons between sites at similar distances [*Wang et al.*, 2007; *Bokoye et al.*, 2007].

[35] From Table 2, the mean difference for the entire data set of daily averaged values between Gibraltar and San Fernando is −0.06 cm (−2.9%), whereas the monthly differences (see Table 3) vary from winter to summer. In winter the San Fernando values are about 8% larger than the Gibraltar values. In summer there is a minimum difference of ~2% between the two. The total difference between El Arenosillo and San Fernando is about −0.14 cm (−6.7%). From Table 3 (monthly values) the differences vary from +5% in summer, when PWV values of El Arenosillo are higher, to −14% in winter. In general the best agreement among the sites is found in summer.

[36] The comparison of differences between Gibraltar and San Fernando for the 0000 UTC data indicates small differences, with a bias of −0.03 cm, and the relative bias histogram (Figure 7) presents Gaussian behavior that indicates nonsystematic differences. However, the 1200 UTC data have a considerably larger bias (−0.14 cm) and the histogram of differences appears shifted toward negative values. This behavior has been noticed by other authors [*Li et al.*, 2003; *Miloshevich et al.*, 2006], with the explanation that it is the result of solar heating of the RS90 sonde during the day, which does not occur at night. This problem is most likely responsible for the observed differences at 1200 UTC, although it must be noted that the bias is of similar amplitude of the diurnal cycle, therefore the contribution of local effects cannot be completely discarded. It must also be noted that the GPS data may have a bias related to the relative calibration of the antenna phase center variations before November 2006 [*Ortiz de Galisteo et al.*, 2010], which is about 0.2 cm. After this correction, the differences San Fernando–Gibraltar would likely increase.

[37] Figure 8 represents the evolution of monthly relative differences over the entire study period. Using this figure, the comparison is more illustrative than in Figure 4 and Table 3, because it highlights some time periods of clear disagreement between El Arenosillo (SP) and the other 2 sites. These periods correspond to the last months of operation of SP numbers 114, 50 and 45b. However, in 2002 the Cimel 45 measurements show similar behavior than the other sites. Figure 8 also shows that the differences between Gibraltar and San Fernando do not exceed 10% except for the first semester

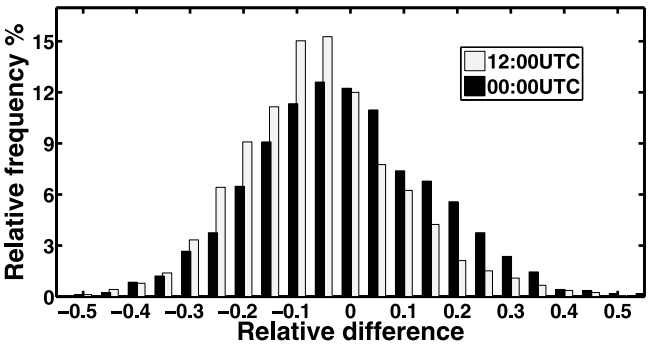

Figure 7. Relative frequency histograms of the relative differences or bias between the data from San Fernando and Gibraltar for the observations at 1200 UTC (white bars) and 0000 UTC (black bars).

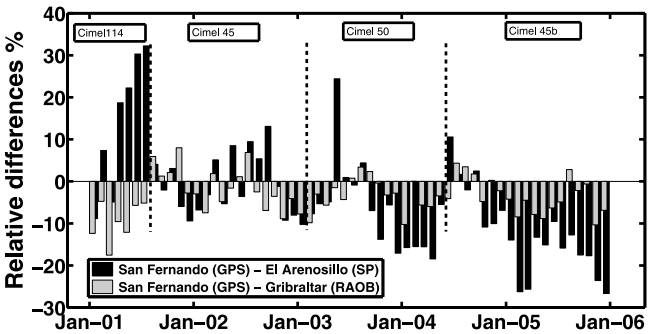

Figure 8. Relative bias of monthly means during the study period, 2001–2005, between the data obtained in San Fernando (GPS) and the other two stations: El Arenosillo (SP) (black bars) and Gibraltar (RAOB) (shaded bars).

Table 4. Summary of the Statistical Comparison Between El Arenosillo and San Fernando Data for Each Sun Photometer Deployed at El Arenosillo Station Analyzed for a Defined Range of Water Vapor Values and for Total Values

AERONET Number–Sun Photometer	Range	Data	RMSE (cm)	RMAD (%)	Bias (cm)
114 Slope (1/d) $(1.8 \pm 0.2) \times 10^{-3}$	0–0.5	0	0.00	0.00	0.00
	0.5–1.5	205	0.45	0.28	0.31
	1.5–2.5	351	0.67	0.29	0.52
	2.5–3.5	37	0.71	0.21	0.53
	3.5–4.5	4	1.05	0.25	1.04
	Total	597	0.61	0.28	0.45
45 Slope (1/d) $(6.9 \pm 5.8) \times 10^{-5}$	0–0.5	0	0.00	0.00	0.00
	0.5–1.5	382	0.24	0.15	0.04
	1.5–2.5	726	0.37	0.14	0.10
	2.5–3.5	271	0.40	0.11	0.015
	3.5–4.5	24	0.38	0.07	0.003
	Total	1403	0.35	0.14	0.07
50 Slope (1/d) $(-5.0 \pm 0.6) \times 10^{-4}$	0–0.5	0	0.00	0.00	0.00
	0.5–1.5	332	0.24	0.17	−0.06
	1.5–2.5	858	0.37	0.15	−0.004
	2.5–3.5	362	0.46	0.12	−0.08
	3.5–4.5	9	0.57	0.12	−0.43
	Total	1561	0.37	0.14	−0.03
45b Slope (1/d) $(-5.5 \pm 0.4) \times 10^{-4}$	0–0.5	7	0.19	0.36	−0.14
	0.5–1.5	525	0.29	0.21	−0.17
	1.5–2.5	1257	0.41	0.16	−0.12
	2.5–3.5	680	0.50	0.14	−0.22
	3.5–4.5	37	0.68	0.15	−0.54
	Total	2506	0.42	0.17	−0.16
All	0–0.5	7	0.19	0.36	−0.14
	0.5–1.5	1444	0.30	0.20	−0.02
	1.5–2.5	3192	0.43	0.17	0.03
	2.5–3.5	1350	0.48	0.13	−0.11
	3.5–4.5	74	0.61	0.13	−0.27
	Total	6067	0.42	0.17	–0.016

2001, the period when the RS80 radiosonde was used, as it was indicated in section 2.

[38] As a summary, the three locations show a very similar pattern, with high correlation and similar seasonal behavior in the PWV data, with differences around 10% that are larger in winter. However, the most noticeable result of this analysis is that the differences between El Arenosillo and the other two sites are largely related to the change of SP instruments. Further, the highest values of these differences are attained at the end of each SP operation period, reaching values up to 20% (end of Cimel 50) and up to 30% (end of 114 and 45b), evidently indicating drift due to aging of the SP filters and other calibration problems [*Halthore et al.*, 1997], as we analyze in the next section.

4.3. Observation of Sun Photometer Drift

[39] As shown above, the differences San Fernando–El Arenosillo (Figure 8) are directly related to the replacement of SP instruments. This implies that a systematic error associated to each particular instrument is affecting the SP observations. Bear in mind that systematic errors, like miscalibration, do not compensate through averaging.

[40] These differences have been calculated for the first and last months of operation of each Sun photometer. The result is that, at the 95% confidence level, the absolute differences in the last 6 months of each SP (0.38 ± 0.30 cm) are significantly larger than those of the previous months (0.27 ± 0.24 cm). Therefore the departure of SP calibration is the reason for the differences between El Arenosillo and San Fernando to be larger than the expected regional variability (around 10%), and clearly depend on the accuracy and stability of each SP calibration. All PWV data of AERONET SPs used in this study attained quality level 1.5, but did not reach level 2.0, due to calibration problems (SP 114 [*Toledano et al.*, 2007a; *Cachorro et al.*, 2008b]), or because the SP does not satisfy network requirements for missing specific filter response [*Holben et al.*, 1998]. All the instruments except SP 114 attained level 2.0 for aerosol optical depth values [*Cachorro et al.*, 2008a, 2008b].

[41] In order to assess possible filter degradation due to aging or a general miscalibration of the SPs, Table 4 shows a comparison with San Fernando for each deployed SP for all data and for the different ranges of water vapor values. For example, SP 45, with a RMSE of 0.35 cm, a bias of 0.07 cm (as defined in the appendix) and a relative mean absolute difference RMAD of 14%, has the best agreement, whereas SP 114 has the worst, with a RMSE of 0.61 cm, a bias of 0.45 cm and a RMAD of 28%. As mentioned, the SP 114 was noted to have a serious calibration problem. Another large monthly difference occurred in May 2003 for Cimel 50 (Figure 8), but in this case the differences arise because the SP was out of order for 15 days during this month. The comparison, depending on water vapor values is also illustrated in Table 4 for all SPs [*Torres*, 2007]. In general, the RMSE increases and the RMAD decreases (with the exception of SP 114) with increasing PWV.

[42] The time series of the relative bias based on daily values is shown in Figure 9 for SP 45 and 114, respectively, and it is also registered in Table 4 for all instruments. The relative bias of SP 114 versus San Fernando shows a linear

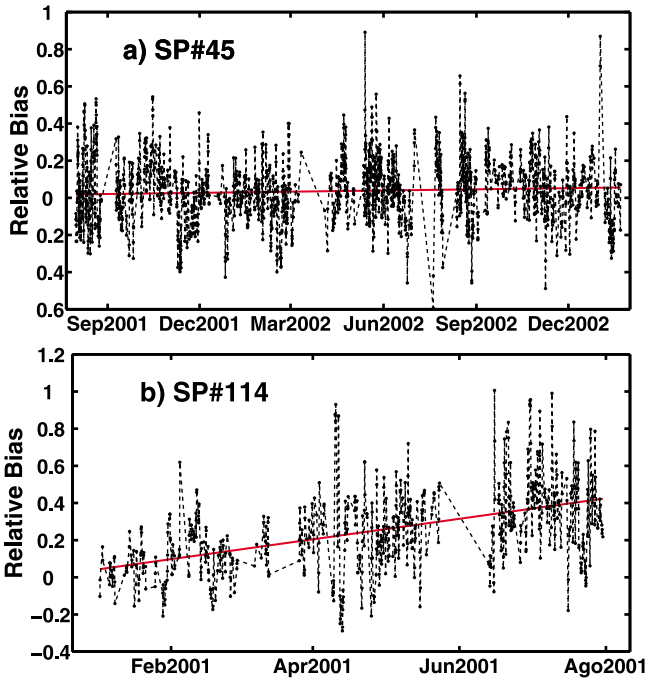

Figure 9. Daily relative bias between San Fernando and El Arenosillo and the regression line of tendency in the periods of the Sun photometers: (a) SP 45 and (b) SP 114.

trend with a slope of $s = (1.8 \pm 0.2)\cdot 10^{-3}$ d^{-1}. This large time dependence is 100 times larger than for SP 45, which has a slope $s = 6.9\ 10^{-5}$ d^{-1}. This means that after 500 days of measurements, SP 45 shows differences of only 2%–3%, while for SP114, after only 200 days, the increase of the relative bias is about 40% (the data from 2000 are not included in this study). SP 50 and 45b have negative slopes and are about 10 times larger than in the case of SP 45, which means that in the same period the variability of the instruments in terms of PWV is approximately 20%.

[43] Nevertheless, the results presented in section 4.2 show that the SP data can be used to characterize the major seasonal features of the PWV (Figure 4) on the basis of monthly means. However, some precaution about possible instrumental malfunction needs to be considered, especially if short periods are analyzed.

4.4. Comparison Between GPS and MODIS

[44] In order to provide an insight about satellite performance for PWV determination over this area, the MODIS near-infrared (NIR) water vapor product MOD05 (collection 5) has been analyzed and compared with our reference data set at San Fernando (GPS) for the same period, i.e., 2001–2005. The NIR MODIS PWV retrieval is based on the transmission in the 940 nm absorption band and the transmission at two window channels (870 and 1240 nm) to derive water vapor [*Gao and Kaufman*, 2003]. These authors report an error of the derived PWV of 10%, that can be larger for retrievals over dark surfaces or under hazy conditions.

[45] For this comparison, a 5 km area around San Fernando has been defined. PWV values of cloud-free MODIS pixels within this area are averaged (typically 50 to 70 pixels at 1 km resolution). In addition only days presenting 50% of cloud-free pixels are taken into account for comparison with GPS data at overpass time ±1 hour.

[46] The multiannual means of the NIR product are shown in Figure 4, together with the ground-based instruments. In general the NIR water vapor from MODIS slightly overestimates GPS data in summer (+5 to +8% difference), but underestimates water vapor in winter by −23%. The differences MODIS-GPS are also indicated in Table 3. The correlation GPS-MODIS NIR (cloud-free cases) is $R^2 = 0.88$ (N = 784 pairs) with slope 1.09 and intercept −0.10 cm, that indicates overestimation by MODIS for high PWV values and underestimation for low values. Similar results are found by *Li et al.* [2003] at HERS (England) and a number of GPS stations in Germany. *Prasad and Singh* [2009] found overestimation by MODIS for all PWV values, although with similar slope and correlation as we report here. In cloudy cases MODIS shows no correlation with GPS and clearly underestimates the PWV [see also *Prasad and Singh*, 2009].

5. Conclusions

[47] The precipitable water vapor content has been studied in the Cadiz Gulf area by means of data available at three locations equipped with different instrumentation (GPS, Radiosondes and AERONET Sun photometer). This study provides the first long-term characterization of PWV over southwestern Europe. The area shows the seasonal behavior of midlatitude zones, with maximum PWV in summer (about 2.6 cm) and minimum in winter (1.4 cm). Remarkable result is the local minimum occurring in July, which may be attributed to the frequent desert dust intrusions occurring over south Spain.

[48] The differences among the three sites range between 10% and 30% on a monthly basis. In some cases differences cannot only be explained by natural variability and are identified as instrumental issues. To verify this, GPS data have been used as a reference. Differences larger than 10% between El Arenosillo (SP) and San Fernando (GPS) appear clearly related to drift in Sun photometer retrievals, due to filter degradation or other calibration problems. For this reason, caution needs to be exercised when using water vapor data from Sun photometer in future analysis, especially if short periods are analyzed. Another instrumental issue is the known problem of sonde heating by sun radiation. Furthermore, the colocated comparison GPS-MODIS indicates high correlation ($R^2 = 0.88$) for cloud-free cases, overestimation by MODIS for high PWV values (summer) and underestimation for low values (winter).

Appendix

[49] Several statistical indicators have been used: RMSE, bias, etc., for our analysis of the PWV differences between the different techniques GPS, SP and Radiosonde. Because sometime certain differences appear in the bibliography about the definition or use, here the expressions taken by us (SP is replace by Radiosonde when the other difference is analyzed). Bear in mind that we are analyzing differences and not the error of a quantity and that GPS data have been taken as the reference value.

[50] The root mean square is

$$\mathrm{RMSE} = \sqrt{\frac{\sum_{i=1}^{N}\left(w_i^{(\mathrm{SP})} - w_i^{(\mathrm{GPS})}\right)^2}{N}}.$$

The bias (or mean difference) and the relative bias are

$$\mathrm{bias} = \frac{\sum_{i=1}^{N}\left(w_i^{(\mathrm{SP})} - w_i^{(\mathrm{GPS})}\right)}{N}$$

$$\text{relative bias} = \frac{\sum_{i=1}^{N}\left(\frac{w_i^{(\mathrm{SP})} - w_i^{(\mathrm{GPS})}}{w_i^{(\mathrm{GPS})}}\right)}{N},$$

respectively. The relative mean absolute difference, RMAD, is

$$\mathrm{RMAD} = \frac{\sum_{i=1}^{N}\left(\frac{\left|w_i^{(\mathrm{SP})} - w_i^{(\mathrm{GPS})}\right|}{w_i^{(\mathrm{GPS})}}\right)}{N}.$$

[51] **Acknowledgments.** The authors gratefully acknowledge the AERONET and PHOTONS teams for their technical support and advice and the staff at San Fernando and Gibraltar stations. Special thanks are due to the people of INTA–El Arenosillo for the maintenance of the Cimel Sun photometer. This work was funded by CICYT under projects CGL2005-05693-C03/CLI and CGL2008-05939-C03-01/CLI and by Junta de Castilla y León under reference GR220. This work was also supported (N.L.) by the Office of Science, U.S. Department of Energy (DOE), under contract DE-AC06-76RLO 1830. Pacific Northwest Laboratory is operated for the DOE by Battelle Memorial Institute.

References

AGU (1995), *Water Vapor in the Climate System*, special report, AGU, Washington, D. C.

Arbelo, M., F. J. Exposito, and F. Herrera (1995), Comparison of total water vapor content obtained from TOVS-NOAA with radiosoundings data in Canary Islands zone, *Proc. SPIE*, *2582*, 178–184.

Bevis, M., S. Businger, T. A. Herring, C. Rocken, R. A. Anthes, and R. H. Ware (1992), GPS meteorology: Remote sensing of atmospheric water vapor using the Global Positioning System, *J. Geophys. Res.*, *97*, 15,787–15,801.

Bokoye, A. I., A. Royer, P. Cliche, and N. O'Neill (2007), Calibration of Sun radiometer based atmospheric water vapor retrievals using GPS meteorology, *J. Atmos. Oceanic Technol.*, *24*, 964–979, doi:10.1175/JTECH2011.1.

Bruegge, C. J., J. E. Conel, R. O. Green, J. S. Margolis, R. G. Holm, and G. Toon (1992), Water vapor column abundance retrievals during FIFE, *J. Geophys. Res.*, *97*, 18,759–18,768.

Buehler, S. A., M. Kuvatov, V. O. John, M. Milz, B. J. Soden, and J. Notholt (2008), An upper tropospheric humidity data set from operational satellite microwave data, *J. Geophys. Res.*, *113*, D14110, doi:10.1029/2007JD009314.

Burrows, J. P., et al. (1999), Global Ozone Monitoring Experiment (GOME): Mission concept and first scientific results, *J. Atmos. Sci.*, *56*, 151–175, doi:10.1175/1520-0469(1999)056<0151:TGOMEG>2.0.CO;2.

Byun, S. H., Y. Bar-Serve, and G. Gent (2005). The new tropospheric product of the International GNSS Service, paper presented at the 2005 ION GNSS Conference, Inst. of Navig., Long Beach, Calif.

Cachorro, V. E., A. M. De Frutos, and J. L. Casanova (1987), Absorption by oxygen and water vapor in the real atmosphere, *Appl. Opt.*, *26*, 501–505, doi:10.1364/AO.26.000501.

Cachorro, V. E., P. Utrillas, R. Vergaz, P. Duran, A. M. de Frutos, and J. A. Martinez-Lozano (1998), Determination of the atmospheric-water-vapor content in the 940-nm absorption band by use of moderate spectral-resolution measurements of direct solar irradiance, *Appl. Opt.*, *37*, 4678–4689, doi:10.1364/AO.37.004678.

Cachorro, V. E., C. Toledano, A. Berjon, A. M. de Frutos, M. Sorribas, and N. S. Laulainen (2008a), An "in situ" calibration correction procedure (KCICLO) based on AOD diurnal cycle: Comparative results between AERONET and reprocessed (KCICLO method) AOD-alpha data series at El Arenosillo (Spain), *J. Geophys. Res.*, *113*, D02207, doi:10.1029/2007JD009001.

Cachorro, V. E., C. Toledano, A. Berjon, A. M. de Frutos, B. Torres, M. Sorribas, and N. S. Laulainen (2008b), An "in situ" calibration-correction procedure (KCICLO) based on AOD diurnal cycle: Application to AERONET El Arenosillo (Spain) AOD data series, *J. Geophys. Res.*, *113*, D12205, doi:10.1029/2007JD009673.

Curier, R. L., J. P. Veefkind, R. Braak, B. Veihelmann, O. Torres, and G. de Leeuw (2008), Retrieval of aerosol optical properties from OMI radiances using a multiwavelength algorithm: Application to western Europe, *J. Geophys. Res.*, *113*, D17S90, doi:10.1029/2007JD008738.

De Tomasi, F., and M. R. Perrone (2003), Lidar measurement of tropospheric water vapor and aerosols profiles over southern Italy, *J. Geophys. Res.*, *108*(D9), 4286, doi:10.1029/2002JD002781.

Duan, J., et al. (1996), GPS meteorology: Direct estimation of the absolute value of precipitable water, *J. Appl. Meteorol.*, *35*, 830–838, doi:10.1175/1520-0450(1996)035<0830:GMDEOT>2.0.CO;2.

Elliott, W. P., and D. J. Gaffen (1991), On the utility of radiosonde humidity archives for climate studies, *Am. Meteorol. Soc.*, *72*, 1507–1520, doi:10.1175/1520-0477(1991)072<1507:OTUORH>2.0.CO;2.

Estellés, V., J. A. Martinez-Lozano, M. P. Utrillas, and M. Campanelli (2007), A columnar aerosol property in Valencia (Spain) by ground-based Sun photometry, *J. Geophys. Res.*, *112*, D11201, doi:10.1029/2006JD008167.

Ferrare, R., et al. (2000), Comparison of aerosol optical properties and water vapor among ground and airborne lidars and Sun photometers during TARFOX, *J. Geophys. Res.*, *105*, 9917–9933, doi:10.1029/1999JD901202.

Flamant, C., J. Pelon, L. Eymard, and J. Tournadre (2003), SSM/I integrated water vapor content measurements in coastal regions: A comparison with shipborne and airborne remote sensing measurements, radiosonde measurements, and NWP model retrievals, *J. Geophys. Res.*, *108*(C3), 8056, doi:10.1029/2001JC001068.

Gao, B. C., and Y. J. Kaufman (2003), Water vapor retrieval using Moderate Resolution Imaging Spectrometer (MODIS) near-IR channels, *J. Geophys. Res.*, *108*(D13), 4389, doi:10.1029/2002JD003023.

Gendt, G. (1998), IGS combination of tropospheric estimates—The Pilot Project, in *IGS 1997 Technical Reports*, edited by I. Mueller et al., pp. 265–269, Jet Propul. Lab., Pasadena, Calif.

Gettelman, A., W. D. Collins, E. J. Fetzer, A. Eldering, F. W. Irion, P. B. Duffy, and G. Bala (2006), Climatology of upper-tropospheric relative humidity from the atmospheric infrared sounder and implications for climate, *J. Clim.*, *19*, 6104–6121, doi:10.1175/JCLI3956.1.

Guanter, L., L. Gomez-Chova, and J. Moreno (2008), Coupled retrieval of aerosol optical thickness, columnar water vapor and surface reflectance maps from ENVISAT/MERIS data over land, *Remote Sens. Environ.*, *112*, 2898–2913, doi:10.1016/j.rse.2008.02.001.

Halthore, R. N., T. F. Eck, B. N. Holben, and B. L. Markham (1997), Sun photometric measurements of atmospheric water vapor column abundance in the 940-nm band, *J. Geophys. Res.*, *102*, 4343–4352, doi:10.1029/96JD03247.

Holben, B. N., et al. (1998), AERONET—A federated instrument network and data archive for aerosol characterization, *Remote Sens. Environ.*, *66*, 1–16, doi:10.1016/S0034-4257(98)00031-5.

Holben, B. N., et al. (2001), An emerging ground-based aerosol climatology: Aerosol optical depth from AERONET, *J. Geophys. Res.*, *106*, 12,067–12,097, doi:10.1029/2001JD900014.

Ingold, T., B. Schmi, C. Mätzler, P. Demoulin, and N. Kämpfer (2000), Modeled and empirical approaches for retrieving columnar water vapor from solar transmittances measurements in 0.72, 0.82 and 0.94 um absorption bands, *J. Geophys. Res.*, *105*, 24,327–24,343, doi:10.1029/2000JD900392.

Intergovernmental Panel on Climate Change (2007), *IPCC Fourth Assessment Report. Working Group I Report: The Physical Science Basis*, Cambridge Univ. Press, Cambridge, U. K.

Lang, R., S. Casadio, A. N. Maurellis, and M. G. Lawrence (2007), Evaluation of the GOME water vapor climatology 1995–2002, *J. Geophys. Res.*, *112*, D17110, doi:10.1029/2006JD008246.

Li, Z., J. Muller, and P. Cross (2003), Comparison of precipitable water vapor derived from radiosonde, GPS, and moderate-resolution imaging spectroradiometer measurements, *J. Geophys. Res.*, *108*(D20), 4651, doi:10.1029/2003JD003372.

Liljegren, J., S. A. Boukaraba, K. Cadi-Pereira, and S. A. Clough (1999), A comparison of integrated water vapor from microwave radiometer, balloon-borne sounding system and Global Positioning System, paper presented at the Ninth ARM Science Team Meeting, U.S. Dept. of Energy, San Antonio, Tex.

Lindenbergh, R., M. Keshin, and H. Van der Marel (2008), High resolution spatio-temporal water vapor mapping using GPS and MERIS observations, *Int. J. Remote Sens.*, *29*, 2393–2409, doi:10.1080/01431160701436825.

Liu, X., D. K. Zhou, A. Larar, W. L. Smith, and P. Schluessel (2008), Atmospheric property retrievals from infrared atmospheric sounding interferometer (IASI), *Proc. SPIE*, *7107*, 71070E, doi:10.1117/12.800361.

Machol, J. L., T. Ayers, K. T. Schwenz, K. W. Koenig, R. M. Hardesty, C. J. Senff, M. A. Krainak, J. B. Abshire, H. E. Bravo, and S. P. Sandberg (2004), Preliminary measurements with an automated compact differential absorption lidar for profiling water vapor, *Appl. Opt.*, *43*, 3110–3121, doi:10.1364/AO.43.003110.

Michalsky, J. J., J. C. Liljegren, and L. C. Harrison (1995), Comparison of Sun photometer derivations of total column water vapor and ozone to standard measures of same at the Southern Great Plains Atmospheric Radiation Measurement site, *J. Geophys. Res.*, *100*, 25,995–26,003, doi:10.1029/95JD02706.

Miloshevich, L. M., H. Vömel, D. N. Whiteman, B. M. Lesht, F. J. Schmidlin, and F. Russo (2006), Absolute accuracy of water vapor measurements from six operational radiosonde types launched during AWEX-G and implications for AIRS validation, *J. Geophys. Res.*, *111*, D09S10, doi:10.1029/2005JD006083.

Niell, A. E., A. J. Coster, F. S. Solheim, V. B. Mendes, P. C. Toor, R. B. Langley, and C. A. Upham (2001), Comparison of measurements of atmospheric wet delay by radiosonde, water vapor radiometer, GPS, and VLBI, *J. Atmos. Oceanic Technol.*, *18*, 830–850, doi:10.1175/1520-0426(2001)018<0830:COMOAW>2.0.CO;2.

Noël, S., M. Buchwitz, H. Bovensmann, and J. P. Burrows (2005), Validation of SCIAMACHY AMC-DOAS water vapour columns, *Atmos. Chem. Phys.*, *5*, 1835–1841, doi:10.5194/acp-5-1835-2005.

Noël, S., S. Mieruch, H. Bovensmann, and J. P. Burrows (2008), Preliminary results of GOME-2 water vapour retrievals and first applications in polar regions, *Atmos. Chem. Phys.*, *8*, 1519–1529, doi:10.5194/acp-8-1519-2008.

Ortiz de Galisteo, J. P., V. Cachorro, B. Torres, C. Toledano, and A. De Frutos (2008), Comparative study of column integrated water vapour content measured with different techniques: Radiometric methods, delay of GPS signal and radio-soundings, paper presented at the 35th Annual European Meeting on Atmospheric Studies by Optical Methods, Maynooth, Ireland.

Ortiz de Galisteo, J. P., C. Toledano, V. Cachorro, and B. Torres (2010), Improvement of PWV estimation from GPS due to the absolute calibration of antenna phase center variations, *GPS Solutions*, doi:10.1007/s10291-010-0163-y.

Prasad, A. K., and R. P. Singh (2009), Validation of MODIS Terra, AIRS, NCEP/DOE AMIP-II Reanalysis-2, and AERONET Sun photometer derived integrated precipitable water vapor using ground-based GPS receivers over India, *J. Geophys. Res.*, *114*, D05107, doi:10.1029/2008JD011230.

Revercomb, H. E., et al. (2003), The ARM program's water vapor intensive observation periods: Overview, initial accomplishments, and future challenges, *Bull. Am. Meteorol. Soc.*, *84*, 217–236, doi:10.1175/BAMS-84-2-217.

Rodríguez, S., X. Querol, A. Alastuey, G. Kallos, and O. Kakaliagou (2001), Saharan dust contributions to PM10 and TSP levels in southern and eastern Spain, *Atmos. Environ.*, *35*, 2433–2447, doi:10.1016/S1352-2310(00)00496-9.

Sapucci, L. F., L. A. T. Machado, J. F. G. Monico, and A. Plana-Fattori (2007), Intercomparison of integrated water vapor estimates from multisensors in the Amazonian region, *J. Atmos. Oceanic Technol.*, *24*, 1880–1894, doi:10.1175/JTECH2090.1.

Schmid, B., K. J. Thome, P. Demoulin, R. Peter, C. Mätzler, and J. Sekler (1996), Comparison of modeled and empirical approaches for retrieving columnar water vapor from solar transmittance measurements in the 0.94-m region, *J. Geophys. Res.*, *101*, 9345–9358, doi:10.1029/96JD00337.

Smirnov, A., B. N. Holben, T. F. Eck, O. Dubovik, and I. Slutsker (2000), Cloud screening and quality control algorithms for the AERONET database, *Remote Sens. Environ.*, *73*, 337–349, doi:10.1016/S0034-4257(00)00109-7.

Smirnov, A., B. N. Holben, A. Lyapustin, I. Slutsker, and T. F. Eck (2004), AERONET processing algorithm refinement, paper presented at the AERONET Workshop 2004, El Arenosillo, Spain.

Thome, K. J., B. M. Herman, and J. A. Reagan (1992), Determination of precipitable water vapor from solar transmission, *J. Appl. Meteorol.*, *31*, 157–165, doi:10.1175/1520-0450(1992)031<0157:DOPWFS>2.0.CO;2.

Toledano, C., V. E. Cachorro, M. Sorribas, A. Berjón, B. A. de la Morena, A. M. de Frutos, and P. Gouloub (2007a), Aerosol optical depth and Ångström exponent climatology at El Arenosillo AERONET site (Huelva, Spain), *Q. J. R. Meteorol. Soc.*, *133*, 795–807, doi:10.1002/qj.54.

Toledano, C., V. E. Cachorro, A. M. de Frutos, M. Sorribas, N. Prats, and B. A. de la Morena (2007b), Desert dust events over the south-western Iberian Peninsula in 2000–2005 inventoried with an AERONET Cimel Sun photometer, *J. Geophys. Res.*, *112*, D21201, doi:10.1029/2006JD008307.

Torres, B. (2007), Estudio comparativo y climatologico del vapor de agua en el area del Golfo de Cádiz mediante tres técnicas diferentes: Fotómetros, GPS y radiosondeos, M.S. project, Valladolid Univ., Valladolid, Spain.

Van Baelen, J., J.-P. Aubagnac, and A. Dabas (2005), Comparison of near-real time estimates of integrated water vapor derived with GPS, radiosonde, and microwave radiometer, *J. Atmos. Oceanic Technol.*, *22*, 201–210, doi:10.1175/JTECH-1697.1.

Wang, J., L. Zhang, A. Dai, T. Van Hove, and J. Van Baelen (2007), A near-global, 2-hourly data set of atmospheric precipitable water from ground-based GPS measurements, *J. Geophys. Res.*, *112*, D11107, doi:10.1029/2006JD007529.

Westwater, E. R., D. Cimini, V. Mattioli, A. J. Gasiewski, M. Klein, V. Leuski, and J. S. Liljegren (2006), The 2004 north slope of Alaska Arctic winter radiometric experiment: Overview and highlights, paper presented at MicroRad XX, IEEE, New York.

Whiteman, D. N., et al. (2006), Analysis of Raman lidar and radiosonde measurements from the AWEX-G field campaign and its relation to Aqua validation, *J. Geophys. Res.*, *111*, D09S09, doi:10.1029/2005JD006429.

Y. Bennouna, A. Berjón, V. E. Cachorro, A. M. de Frutos, J. P. Ortiz de Galisteo, C. Toledano, and B. Torres, Group of Atmospheric Optics, University of Valladolid, Prado de la Magdalena s/n, Valladolid ES-47071, Spain. (chiqui@baraja.opt.cie.uva.es)

N. Laulainen, Pacific Northwest National Laboratory, Richland, WA 99352, USA.